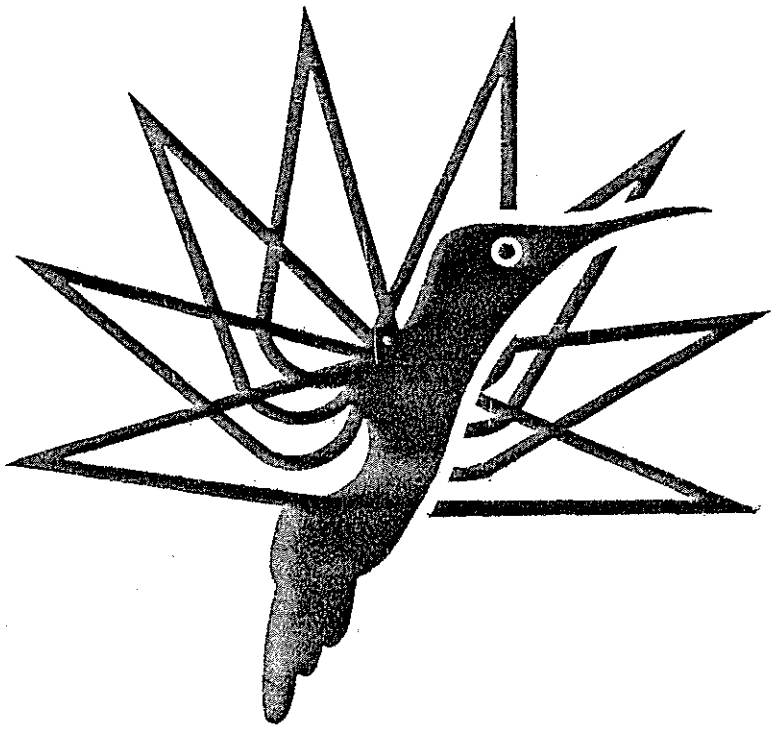

SOME RESULTS OF DYNAMIC MEASUREMENTS WITH A MODEL HINGELESS ROTOR

by

H.J. Langer
Deutsche Forschungs- und Versuchsanstalt für Luft- und Raumfahrt
Braunschweig, Germany

R. Stricker
Messerschmitt-Bölkow-Blohm GmbH
München, Germany
P.O. Box 801140

FIFTH EUROPEAN ROTORCRAFT AND POWERED LIFT AIRCRAFT FORUM
SEPTEMBER 4 – 7TH 1979 - AMSTERDAM, THE NETHERLANDS

SOME RESULTS OF DYNAMIC MEASUREMENTS WITH A MODEL HINGELESS ROTOR +)

H.J. Langer
Deutsche Forschungs- und Versuchsanstalt für Luft- und Raumfahrt
Braunschweig, Germany

R. Stricker
Messerschmitt-Bölkow-Blohm GmbH
München, Germany
P.O. Box 801140

Abstract

A joint experimental program between DFVLR and MBB has been conducted on a 4 m diameter four bladed hingeless rotor in an open 7.4 m by 4.8 m wind tunnel. Similarity between model rotor and full scale Bo 105 rotor was achieved by accord of Mach-, Lock- and Cauchy-number. In order to measure oscillatory rotor loads up to a frequency of 100 Hz, the dynamic lay-out of the rotor balance and its vibrational characteristics are very important.

Data acquisition was made by two PCM data units. Rapid data processing and on-line monitoring of static and dynamic loads at critical components, with comparison to 100 % markings for calculated fatigue allowable loads, is essential for rotor safety and reliable data. Digitized dynamic data were recorded by tape for detailed off-line analysis.

Standard model tests were performed in an equidistant scanned $\mu - \alpha - \Theta_{0.7} - \Theta_S$ domain covering $\mu = 0$ to 0.20, $\alpha = -15$ to $+5$ deg., $\Theta_{0.7}$ corresponding to load factors of $g = 0.5$ to 1.5, and Θ_S to produce shaft moments of $KM/\sigma \approx \pm 0.015$. Results were crossplotted to eliminate data errors. Corrected data may be used to interpolate values for given flight conditions.

Using the thrust and the rotor shaft moment from full scale flight tests as input data, the values of interest (1/REV, 3/REV, 4/REV, 5/REV blade loads and 4/REV hub forces and moments) for level flight were obtained by multidimensional interpolation. Results from model tests were compared with values from full scale flight tests as well as from digital simulation. Trim parameters (KM_{β_1}, $\Theta_{0.7}$, Θ_c, Θ_S) show good agreement apart from some differences in the lateral control angle Θ_c. Blade loads (KM_{β_3}, KM_{β_5}, KM_{ζ_3}, KM_{ζ_5}) agree well, but model data show a shift of the transitional maxima in the direction of higher μ. Model rotor hub moments (KM_{x_4}, KM_{y_4}) differ significantly from full scale results. Calculated results agree more with the values from full scale flight tests than with those from model tests, in cases where the model and flight test data differ significantly.

A possible cause for the differences between model and full scale results may be the rotor wake - wind tunnel interference as well as some imponderables of the rotor balance or some asymmetric properties of the rotor.

+) Work sponsored by the Ministry of Defence of the Federal Republic of Germany

Notation

A	m^2	rotor disc area
c	m	blade chord
KP	-	force coefficient = $2\ P/\rho \cdot V^2 \cdot A \cdot \sigma$
KM	-	moment coefficient = $2\ M/\rho \cdot V^2 \cdot A \cdot R \cdot \sigma$
M_x, M_y, M_z	Nm	hub moments around x,y,z-axis
m	kg	mass
n	-	number of blades
P_x, P_y, P_z	N	hub forces in x,y,z-direction
r	m	radial station
R	m	rotor radius
S	-	scaling factor
V	m/sec	free stream velocity, wind tunnel speed
V_x, V_y, V_z	m/sec	velocity in x,y,z-direction
V_T	m/sec	rotor tip speed
x, y, z	-	rectangular coordinates, rotor fixed, right handed, x forward
α	deg	rotor angle of attack
$\Theta_{0.7}$	deg	collective pitch at r/R = 0.7
Θ_c	deg	lateral control angle
Θ_s	deg	londitudinal control angle
Θ_z	deg	cyclic pitch = $(\Theta_s^2 + \Theta_c^2)^{1/2}$
μ	-	advance ratio = $V/\omega \cdot R$
ρ	kg/m^3	air density
σ	-	solidity = $c \cdot n/\pi \cdot R$
ω	Hz	rotor frequency
ω_β	Hz	flapping frequency
ω_ξ	Hz	lagging frequency

Indices

β	-	flapwise
ξ	-	lagwise
1, 2, 3, 4, 5	-	number of rotor harmonics

1. Introduction

Today's helicopters are used for an ever increasing number of tasks by both civilian and military users. Particulary for military helicopters, there is a continuously increasing need for improving aircraft performance, optimized stability, control behavior, and noise reduction. To satisfy these requirements, much more fundamental knowledge in helicopter aerodynamics, aeroelastics, dynamics, acoustics, and flight mechanics is essential.

In recent years theoretical work in these areas has been intensified. Now it seems to be necessary to verify and expand theoretical results with proper and sufficient testing. To do this job, a helicopter test stand for large wind tunnels was built (Reference 1), following a contract between the German Ministry of Defence and DFVLR, Dornier, MBB and VFW-Fokker. The contract included the building of a Mach-scaled hingeless 4-blade model rotor following the Bo 105 rotor concept, a swashplate and control system, a fuselage model and a fuselage balance, a rotor support and a drive unit, and a data acquisition system. After a construction period of two years and a further two years of testing and calibration of components (References 2 and 3), the rotor was tested over a wide regime (References 4 and 5). Figures 1 and 2 give a view of the model test stand and of the flying full scale version.

The primary objectives of this paper are
- to give a short description of the test stand and of the model in comparison to the full scale rotor (Bo 105),
- to depict the equipment for measuring dynamic rotor loads and the data acquisition system,
- to show some examplary results from standard rotor tests and to give an example of how these results may be used to interpolate data for trimmed level flight, and
- to compare model rotor loads with results from full scale flight tests and digital simulation.

2. Model Hingeless Rotor and Test Stand

2.1. Model Test Stand and Full Scale Rotor (Bo 105)

The model rotor is a Mach-scaled main rotor of the Bo 105. The scale factor of about 2.5 may be considered as a good compromise to obtain satisfactory conformity in tip Re-number and to obtain a rotor small enough to be tested in the largest wind tunnels presently available in Europe.

Figure 3 shows a summary of the scaling parameters. The blade chord e.g. is not exactly scaled in order to improve conformity in Reynolds-number and Lock-number. Owing to the nearly exact Lock-number scaling, an important condition for similarity of blade motion, controlability and damping between the model and the full scale rotor is fulfilled. Testing the model near α = 0 deg., the influence of gravity may be neglected in comparison to the centrifugal forces. Therefore, the difference in Froude-number (model Fr = 49.2, full scale rotor Fr = 31.4) may not be critical, except for the influence on rotor stability. The flapwise and lagwise frequency ratios of the rotor blades are also compared in Figure 3 up to the 4th and 3rd mode. The higher modes show small differences. However, the first lagwise mode of the model was increased to obtain a better safety margin against ground resonance. Owing to the utilization of the same materials for constructing the rotor blades, the Cauchy-number should be the same for the model and the full scale rotor. Therefore, a rather good similarity in blade bending, torsion and blade loads may be expected.

A survey of trimmed 1-g-flight conditions of the Bo 105 in terms of model test stand parameters, angle of attack α and advance ratio μ, is given in Figure 4. The α-boundary restricts the rate of climb/descent to $V_z \approx -8$ to +8 m/sec at μ = 0.20 and this rate is reduced to $V_z = \pm 0$ at μ = 0, cutting off vertical climb/descent. However, level flight may be simulated up to the highest μ.

2.2. Equipment to Measure Dynamic Rotor Loads

A basic demand in designing the rotor test stand was to measure mean values, as well as dynamic rotor forces, moments, and blade loads up to higher rotor harmonics, with sufficient accuracy. In building up the rotor support system and assembling/testing the components of the test stand, there arose considerable difficulties in constructing the rotor balance: It has to measure large static values of rolling/pitching moments and thrust as well as small forces in the x/y-direction and, last but not least, the dynamic parts of the rotor hub forces and moments. The balance should be small in the y-direction in order not to disturb the contour of scaled helicopter fuselages.

Because it is nearly impossible to built a balance free of resonance frequencies in all directions over the entire frequency regime up to the 9th rotor harmonic, exact measurements are not possible through the whole frequency range. Care was taken to avoid resonance peaks at or near $n \cdot \omega_{Ro}$-frequencies (n = 1 to 5). The balance was calibrated only at these frequencies up to the 5th rotor harmonic. Figure 5 gives an example of a calibration procedure. Lateral force P_x is

excited by a noise input and the outputs of one of the seven force transducers is shown. The magnitude of the transfer function shows approximately linear behavior around the n/REV frequencies up to 5th rotor harmonic. The resonance peaks at about 1.5/REV and 0.6/REV should not cause trouble when measuring at rotor harmonic frequencies. At 5/REV the magnitude of the transfer function becomes too small to calibrate higher rotor harmonics. The phase of the transfer function may change rapidly and nonlinearly around some n/REV frequencies, see 2/REV e.g. Therefore, the accuracy of the phase information is restricted to $\Delta\varphi$ = 10 to 20 deg. on average.

Owing to the 5 degrees of freedom (x-/y-/z-forces, x-/y-moments) and the 7 force transducers of the balance (1 in x-, 2 in y-, and 4 in z-direction), the results from rotor balance calibration may be collected in 2 n 7 by 5 matrices (n = number of rotor harmonics) containing the magnitude and phase information of the transfer functions. During data reduction, these matrices may be used to calculate the rotor forces and moments from the measured force transducer outputs, reducing the overdetermined systems of linear equations for each frequency by calculating the least-squares solution.

Rotor blade flapwise and lagwise bending moments were measured near the blade root (r/R = 0.104) by strain gage bridges. Blade torsion was recorded via pitch link loads and the blade angle of attack was surveyed by a potentiometer.

2.3. Data Acquisition

The measured data, from the rotating system (blade and pitch link loads) and the fixed system (rotor balance and accelerometers), are collected in two PCM-lines, Figure 6, each having a transfer capability of 125 Kbit/sec. 16 channels are recorded from both systems. With a resolution of 10 bits, each channel is scanned with a data rate of 390 bit/sec. To avoid aliasing effects when analysing the data, it is recommended to scan about 5 data points every oscillation. This results in an aliasing free frequency of 78 Hz which is approximately the 5th rotor harmonic. Power supply to the sensors, the amplifiers, and A/D converters in the rotating system is provided by a slip ring. A second one is used to transfer the PCM-signal to the ground unit.

To ensure rotor safety, the time signals of the rotor balance, the rotor hub moments, the blade bending moments and the pitch link loads were keyed to the rotor shaft 1/REV signal and monitored by a "quicklook" data system, Figure 6. 100 %-markings were defined for critical components which were not to exceed the calculated fatigue allowable loads. Should a

particularily interesting vibration or load phenomena require an immediate analysis and recording an analysator was on-line. The mean values from the "quicklook" data system were taken and crossplotted to check the quality of the data and to eliminate incorrect data points.

In the dynamic data system, Figure 6, analog data from all channels of the rotating and fixed system are digitized and recorded on magnetic tape. Detailed off-line analysis of the experiments is done using powerful digital computers.

3. Some Results and Discussion

3.1. Results in the $\mu - \alpha - \Theta_{0.7} - \Theta_S$ Domain

Model tests at this time were performed in the advance ratio - angle of attack region from $\mu = 0$ to 0.20 and $\alpha = -15$ to +5 deg. in an open wind tunnel. Collective pitch was varied in steps of $\Delta\Theta_{0.7} = 2$ deg. to cover the load factor range of $g \approx 0.5$ to 1.5. Londitudinal control angle was altered in steps of $\Delta\Theta_S = 1$ deg. to produce shaft moments in the range of $KM/\sigma \approx \pm .015$, i.e. the moment capability of the full scale rotor. Lateral control angle Θ_S was set to trim a rolling moment of $KM_x/\sigma = -0.00015$; a mean value taken from forward flight of the full scale rotor (Reference 5).

Measured data were collected using the data acquisition system shown in Figure 6 and analysed by a digital computer. Special regard was given to the 1/REV, 3/REV, 4/REV and 5/REV blade loads, and the pitch link loads in the rotating system as well as to the 4/REV hub forces and moments in the fixed system. Results were crossplotted to eliminate data errors.

Typical corrected results can be seen from Figure 7. The 1/REV flapwise and lagwise blade bending moments at $\Theta_{0.7} = 6$ deg. and $\Theta_S = -1$ deg. versus μ and α are shown as an example. Crossplots similar to these may be used to interpolate data for any given flight condition that is covered by the $\mu - \alpha - \Theta_{0.7} - \Theta_S$ region explored with the model. An example for interpolation, of level flights between $\mu = 0$ to 0.20, will be given below in comparison with full scale data from flight test and digital simulation.

To check the similarity of the model and the basic full scale rotor (as described in 2.1.), some comparisons were made. For example, one of the primary properties of a rigid rotor, the moment capacities were compared. Figure 8 shows the shaft moment per deg. of cyclic pitch vs. rotor thrust at hover. Agreement between data measured from model and full scale rotor is good and the typical influence of rotor downwash can be noticed.

Peak-to-peak oscillatory blade loads per deg. of cyclic pitch vs. rotor thrust at hover are also shown in figure 8. Whereas the trends of flapwise and lagwise oscillatory bending moments vs. rotor thrust agree well, the deviation of the first lagwise mode of the model ($\bar{\omega}_{\zeta_1} = 0.71$) from the first mode of the full scale rotor ($\bar{\omega}_{\zeta_1} = 0.63$) produces the higher lagwise loads as can be confirmed by calculation. The difference between oscillatory flapwise loads of the model and the full scale rotor, is caused by higher harmonics as can be seen from the shaft moment, representing the 1/REV flapwise moment and being nearly identical for the model and the full scale rotor.

3.2. Model Data Simulating a Level Flight

The model rotor data described above may be used to interpolate data for any flight condition covered by the $\mu - \alpha - \theta_{0.7} - \theta_S$ region measured. For example, the data for a trimmed level flight in comparison to the full scale rotor can be obtained by interpolation using the rotor thrust and the shaft moment from flight measurement as input data.

Figure 9 shows the interpolated values of the control angles for a 'level flight' of the model in comparison to calculated values for the full scale rotor in the $\mu = 0$ to 0.20 region. The collective pitch angles $\theta_{0.7}$ agree very well, except for slightly lower values for the model near $\mu = 0$, caused by ground effect. For the lateral control angle θ_c, the typical relative extremum, owing to rotor downwash effects in transition flight, is shifted from $\mu \approx 0.05$ (full scale) to $\mu \approx 0.10$ (model). This effect may be evoked by the influence of the wind tunnel on the rotor wake geometry and transportation, as well as by some differences in the coupling behavior owing to the 0 deg. coning angle of the model. As may be expected, the 1/REV flapwise blade bending moments, also shown in figure 9, agree well for the model (interpolated) and the full scale rotor (measured and calculated) whereby the phase angle of the model, especially, is represented with good accuracy by the values calculated for the full scale rotor.

3/REV and 5/REV flapwise and lagwise blade bending moments, primarily causing the 4/REV oscillatory hub moments and forces for a four bladed rotor, can be seen from Figure 10. The 3/REV loads generally are about twice as high as the 5/REV loads. The lagwise moments are in reasonable agreement for the model and the full scale rotor, whereas for the flapwise moments the model shows higher 3/REV loads. A general difference between model and full scale rotor results is observable in the shifting of the relative maximum of the loads in the direction of higher advance ratios. This effect seems to be evoked by rotor wake-wind tunnel interference.

The consequence of the 3/REV and 5/REV blade loads discussed above, 4/REV rotor hub oscillatory moments, can be seen from Figure 11. The moments measured from the model are more than twice as high as the moments from full scale flight tests. The relative extremum owing to rotor downwash effects in transition flight is again shifted to higher μ for the results of the model. The phase angles of rolling and pitching moments are in reasonable agreement for the model and the full scale rotor. Calculated 4/REV moments for the full scale rotor, using a semi-empirical downwash model (Reference 6) that simulates especially transition flight effects, agree with the results from full scale flight test rather than from model test. The differences between the moments measured from model and full scale flight test may be caused by rotor wake-wind tunnel interference as well as by difficulties in measuring comparable rotor hub loads.

Crossplots of 3/REV and 5/REV lagwise and flapwise blade bending moments versus 4/REV rotor hub forces and moments for advance ratios of μ = 0.05 to 0.20, are shown in Figure 12. For the influence of the lagwise moments on the hub forces as well as for the influence of the flapwise moments on the hub moments, the 3/REV components dominate and correlation between model and full scale rotor concerning 3/REV blade loads is good. The 5/REV influence of lagwise moments on hub forces appears to be very similar for the model and for the full scale rotor, whereas 5/REV influence of flapwise moments on hub forces is stronger for the full scale rotor than for the model.

A clear view of rotor hub in plane 4/REV oscillatory moments, first and foremost responsible for the vibrational neveau of the four bladed rotor, is given in Figure 13. The ellipses taken from full scale rotor flight tests are relatively narrow because the phase shift between rolling and pitching moment components is near to 0 or 180 deg. respectively. The magnitude of the ellipses increases and decreases versus μ, showing the typical relative extremum at $\mu \approx 0.075$ resulting from transitional downwash effects. The calculated ellipses also demonstrate the relative extremum at low advance ratio and their magnitude is in reasonable agreement with the full scale results. For the model, the ellipses are more circular owing to the phase shift of nearly $\pm$ 90 deg. between rolling and pitching moment. The increase of the magnitude of the ellipses may be compared to the full scale results, but the extremum is met not until about μ = 0.15 and the magnitude of the ellipses decreases very slowly in comparison to the full scale results. Conversely, the phase behavior of the moment motion is in good agreement to that from the full scale rotor. The differences concerning the magnitude of the ellipses seem to be caused by wind tunnel influence on rotor wake geometry and transportation as well as by some characteristics of the measuring equipment for the rotor hub loads and some asymmetric properties of the model rotor.

4. Conclusions

A model rotor of 4 m diameter, Mach-, Lock-, and Cauchy-scaled from a four bladed hingeless rotor of 10 m diameter, may be used to simulate the aerodynamic, dynamic, and aeroelastic behavior of the full scale rotor. An especially developed rotor balance allows the measurement of the rotor harmonic hub forces and moments up to the fifth order.

Rotor safety can be ensured by monitoring the loads of critical components using a "quicklook" data system to prevent exceeding allowable calculated fatigue loads. Mean values taken from the "quicklook" data system and crossplotted, check the quality of the data and help to eliminate incorrect data points. Digitized dynamic data may be recorded by tape for detailed off-line analysis by computer.

Standard tests of the model may be performed in an equidistant scanned $\mu - \alpha - \Theta_{0.7} - \Theta_S$ domain covering the area of interest. The increments of $\Delta\mu = 0.05$, $\Delta\alpha = 5$ deg., $\Delta\Theta_{0.7} = 2$ deg., and $\Delta\Theta_S = 1$ deg. appear to be small enough to obtain the data of interest (1/REV, 3/REV, 4/REV, 5/REV blade loads and 4/REV hub forces and loads for a 4 bladed rotor, for example) of sufficient reliability by interpolation.

Results from standard tests may be used to interpolate the data for a trimmed level flight in comparison to the full scale rotor, for example, using the rotor thrust and the shaft moment from flight test as input data. Comparison of trim parameters (KM_{β_1}, $\Theta_{0.7}$, Θ_c, Θ_S) shows not only the validity of the interpolating process but also certain differences especially in the lateral control angle Θ_c, that may be caused primarily by wind tunnel-rotor wake interference. Model rotor blade loads (KM_{β_3}, KM_{β_5}, KM_{ζ_3}, KM_{β_5}) show rather good agreement except for a shift of the relative maximum (caused by rotor-wake interference) to a higher μ. Model rotor hub moments (KM_{x_4}, KM_{y_4}) show about twice the magnitude of the full scale results and a shift of the maxima, in the direction of higher μ, greater than that shown by the blade loads. As well as the rotor wake-wind tunnel interference, a possible cause for the rather poor agreement of the hub moments, measured from model and full scale rotor, may lay in some imponderables of the rotor balance (that was not calibrated for $\alpha \neq 0$, e.g.) and some asymmetric properties of the rotor. (Experimental and theoretical work is in progress on this task.) Calculated results agree more with the values from full scale flight tests than with those from model tests in cases where the model and flight tests data differ significantly.

5. References

1) B. Gmelin, A Model for Windtunnel Rotorcraft Research Model Design and Test Objectives, presented at 2nd European Rotorcraft and Powered Lift Aircraft Forum, Bückeburg, 1976.

2) H.J. Langer, F. Kiessling, R. Schröder, A Model for Windtunnel Rotorcraft Research - Ground Resonance Investigations, presented at 2nd European Rotorcraft and Powered Lift Aircraft Forum, Bückeburg, 1976.

3) B. Gmelin, H.J. Langer, P. Hamel, DFVLR-Rotorcraft Research, presented at Flight Mechanics Panel Symposium of AGARD on "Rotorcraft Design", NASA Ames, 1977.

4) H.J. Langer, B. Junker, Ergebnisse aus Windkanaluntersuchungen mit dem DFVLR-Rotorversuchsstand, DFVLR, IB 154-78/28,(1978).

5) R. Stricker, V. Mikulla, E. Allramseder, Standard-Erprobung des Forschungs-Modellrotors im Windkanal, einschließlich Modellvergleichen, MBB GmbH, Bericht UD-267-78.

6) R. Stricker, W. Gradl, Rotor Prediction with Different Downwash Models, Paper No. 6 presented at the 4th European Rotorcraft and Powered Lift Aircraft Forum, Stresa, Sept. 1978.

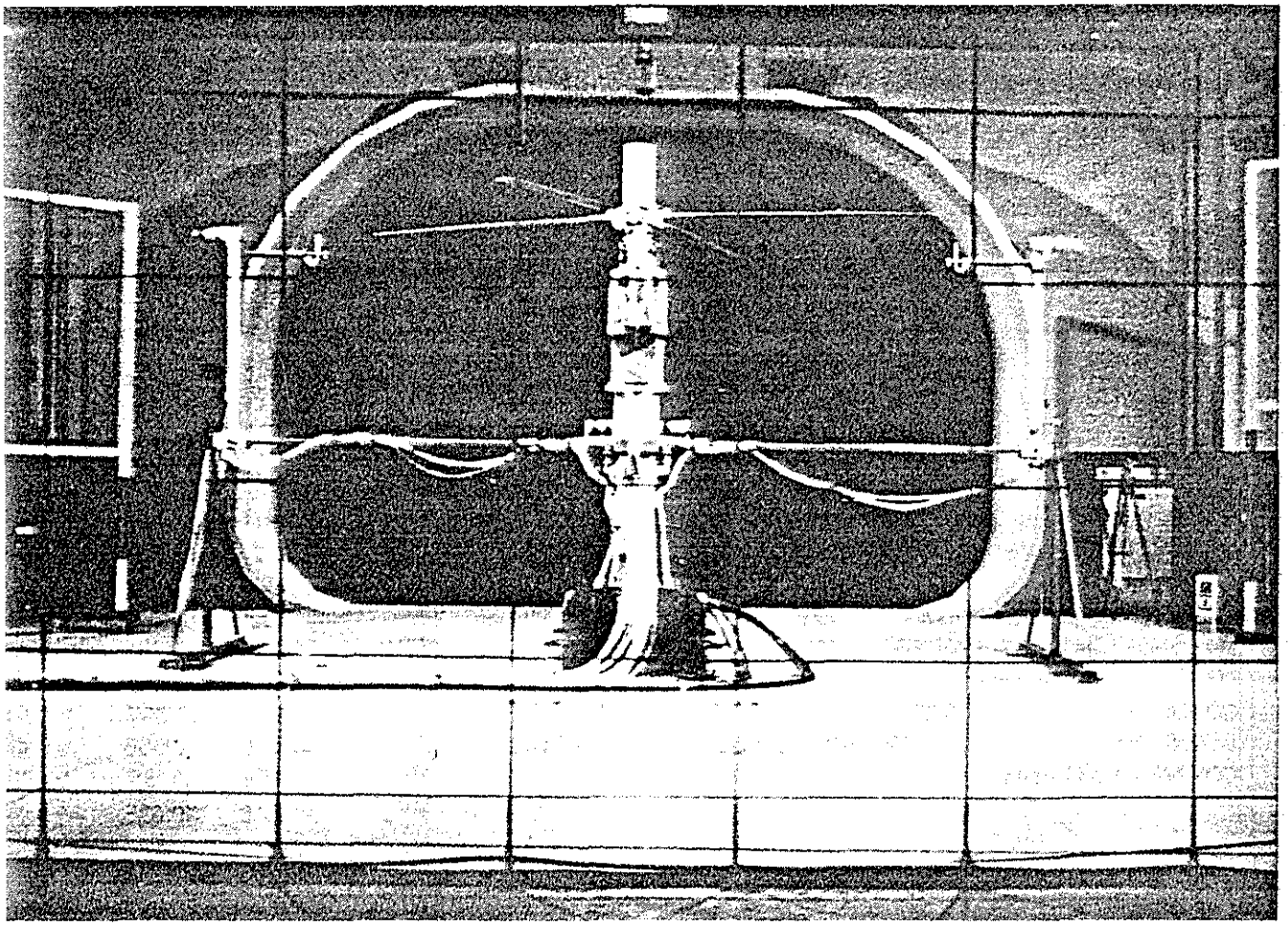

Figure 1: Model rotor test stand

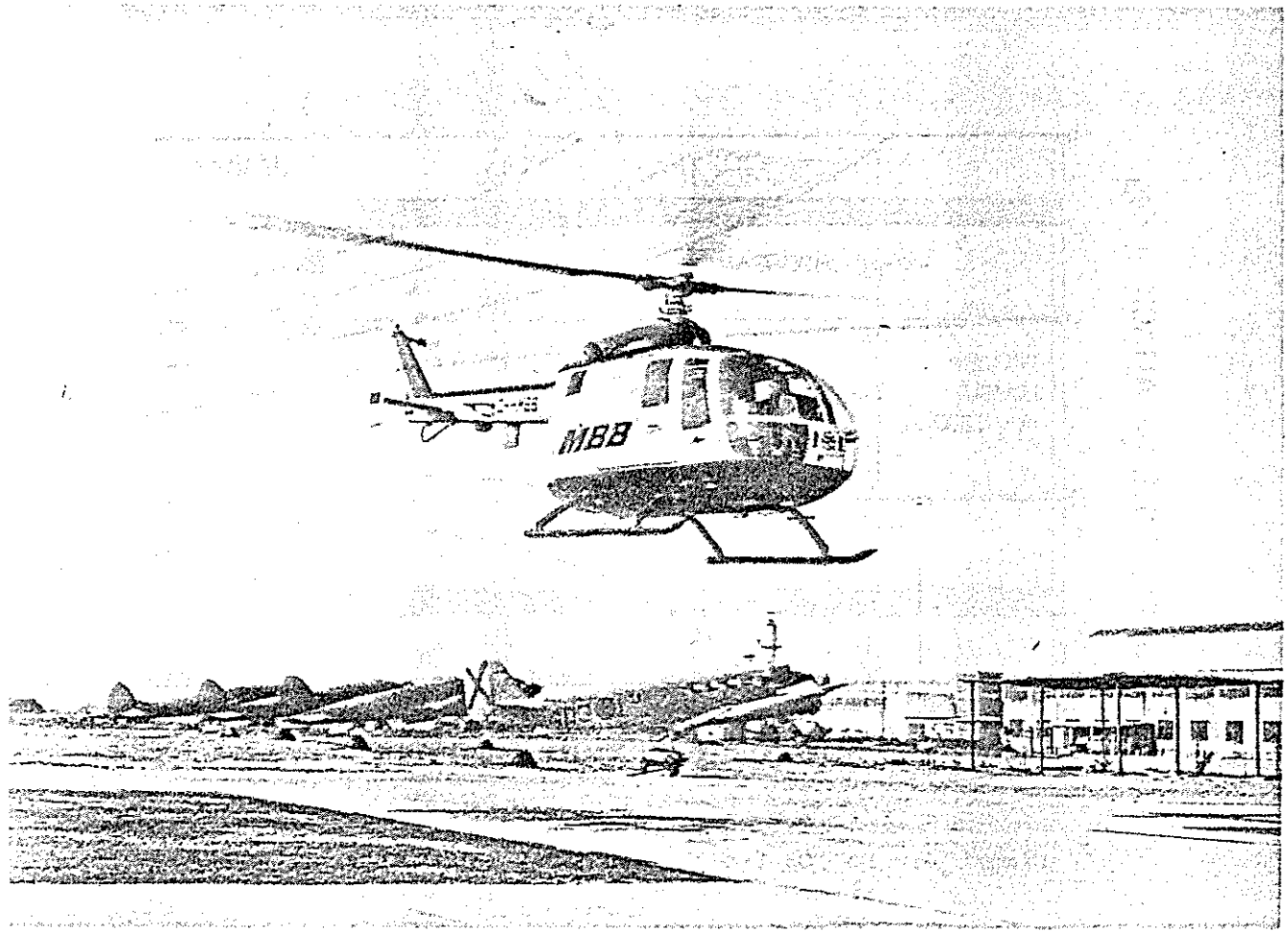

Figure 2: Bo 105 in flight

SCALING FACTOR S = 2.456

	MODEL	BO 105	FACTOR
ROTOR DIAMETER - m	4.00	9.82	s
ROTOR SPEED - rev/min	1040	424	s^{-1}
BLADE CHORD - m	0.121	0.270	0.91 s
BLADE TWIST - deg	-8.	-8.	1
TIP-SPEED - m/s	218	218	1
DESIGN THRUST - daN	374	2256	s^2
MAX. SHAFT MOMENT-daNm	68	1006	s^3
DISC LOADING - daN/m^2	30	30	1
SOLIDITY	0.077	0.070	0.91
BLADE PROFIL	NACA	23012 mod.	
CONING ANGLE - deg	0	2.5	

		MODEL	BO 105	FACTO
TIP MACH-NUMBER		0.64	0.64	1
TIP RE-NUMBER $\cdot 10^{-6}$		1.26	2.82	2.24
LOCK-NUMBER		4.54	4.47	1.01
FROUDE NUMBER		49.2	31.4	0.6
FREQUENCY RATIOS (CALCULATED)				
FLAPWISE	1st	1.122	1.117	0.99
	2nd	2.831	2.751	0.97
	3rd	5.056	4.946	0.97
	4th	7.917	7.837	0.9
LAGWISE	1st	0.716	0.666	0.9
	2nd	4.169	4.139	0.9
	3rd	9.518	10.635	1.11

Figure 3: Scaling parameters of model rotor and Bo 105 rotor

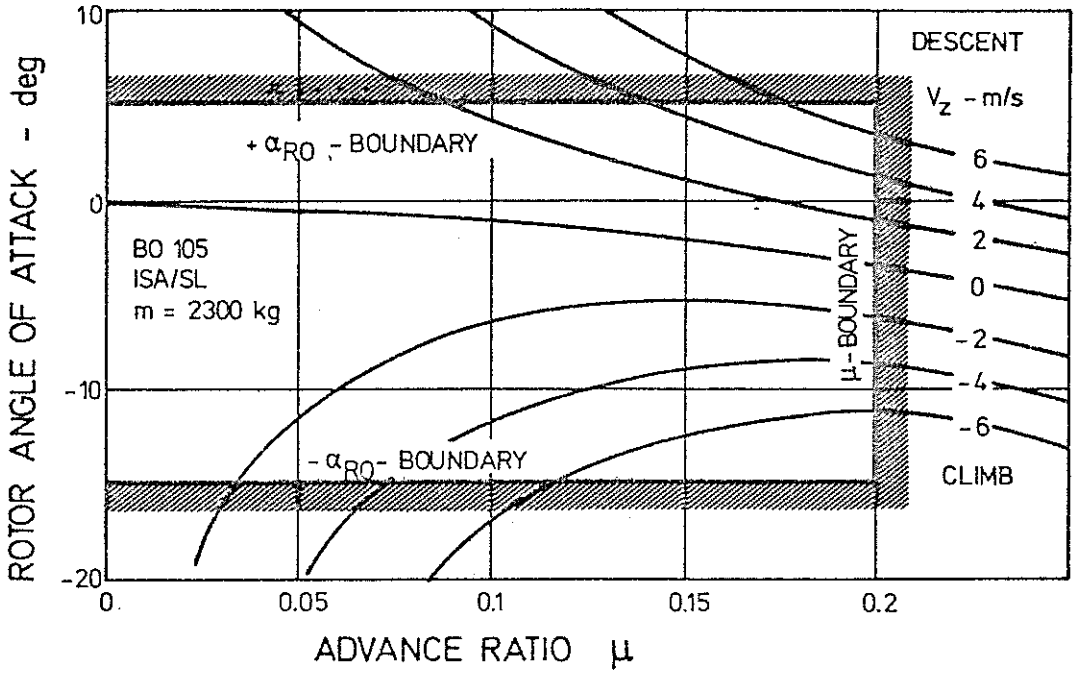

Figure 4: Bo 105 1-g-flight conditions in terms of model rotor parameters μ and α

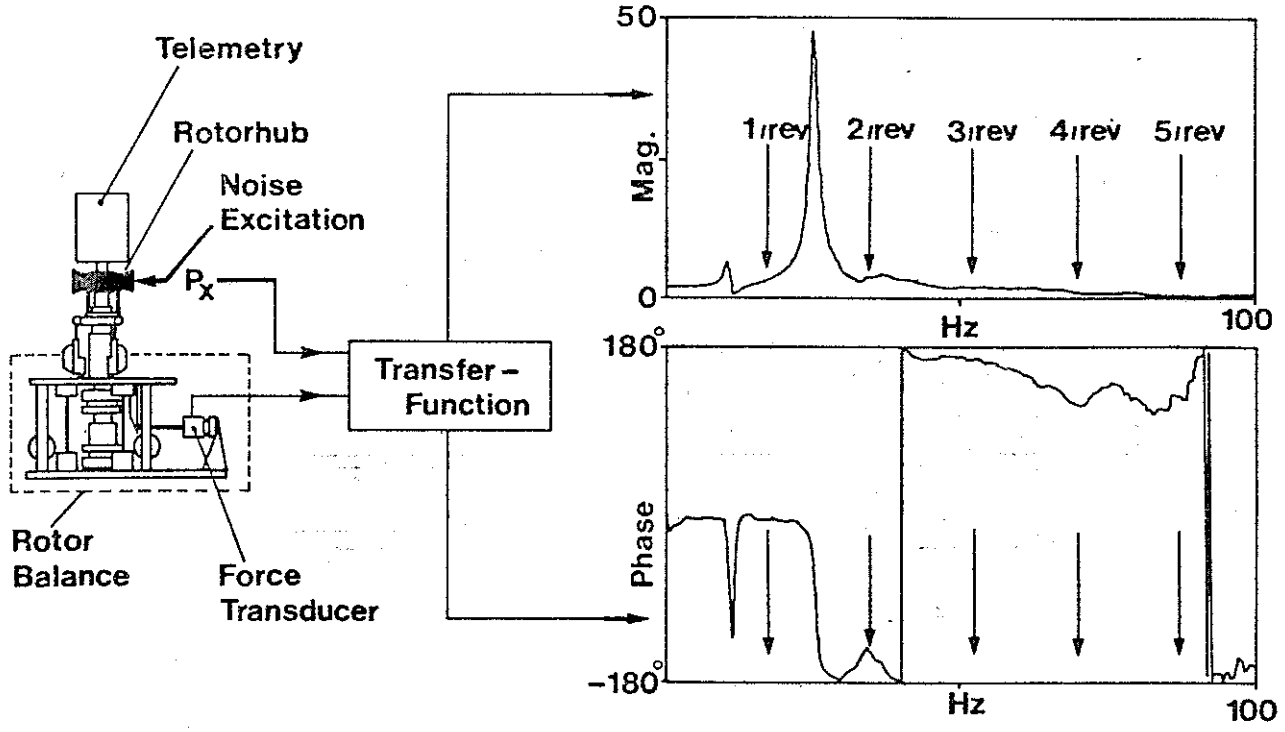

Figure 5: Rotor balance calibration procedure

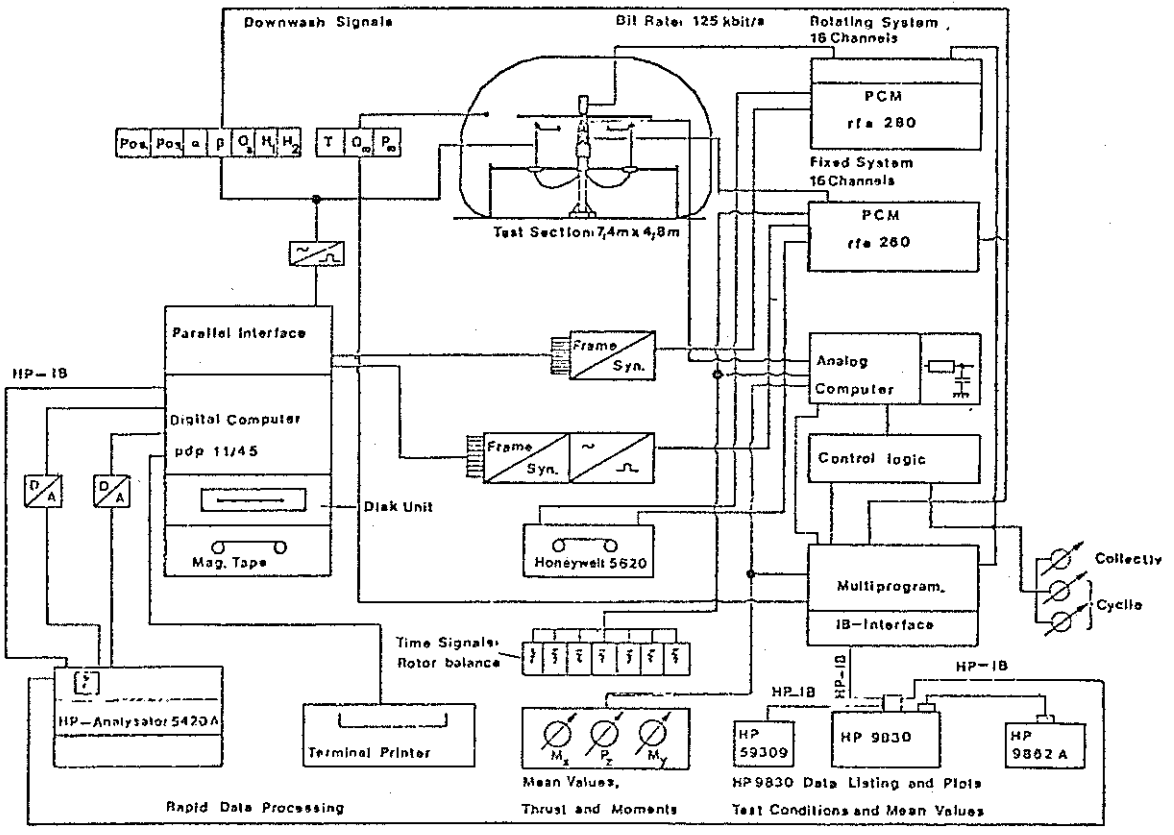

Figure 6: Model rotor test stand data acquisition system

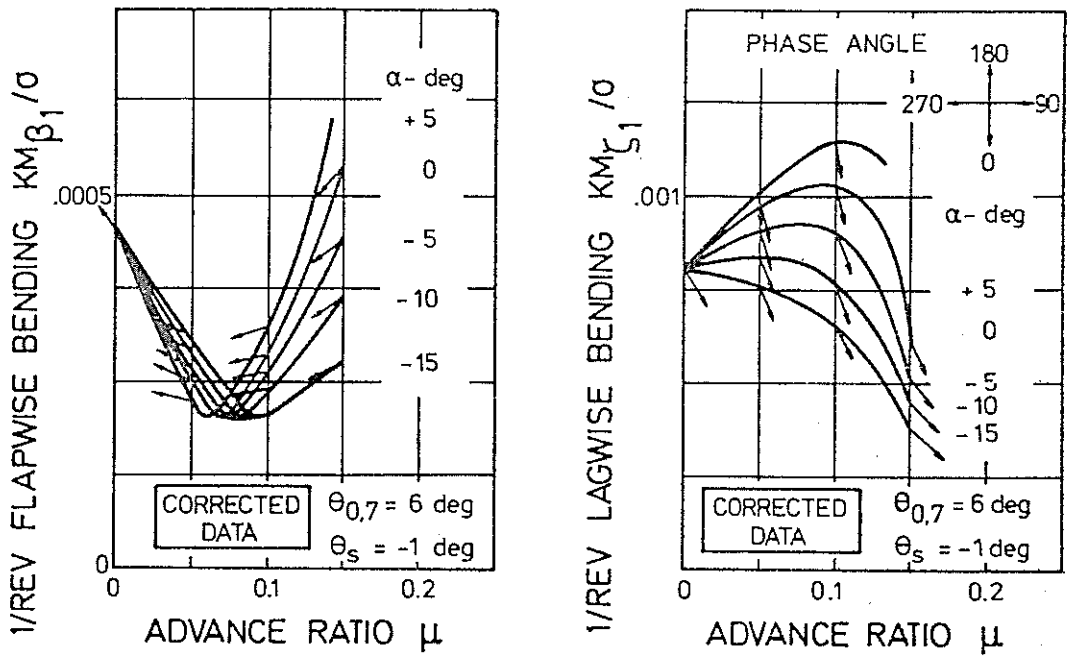

Figure 7: Typical corrected results from model rotor test

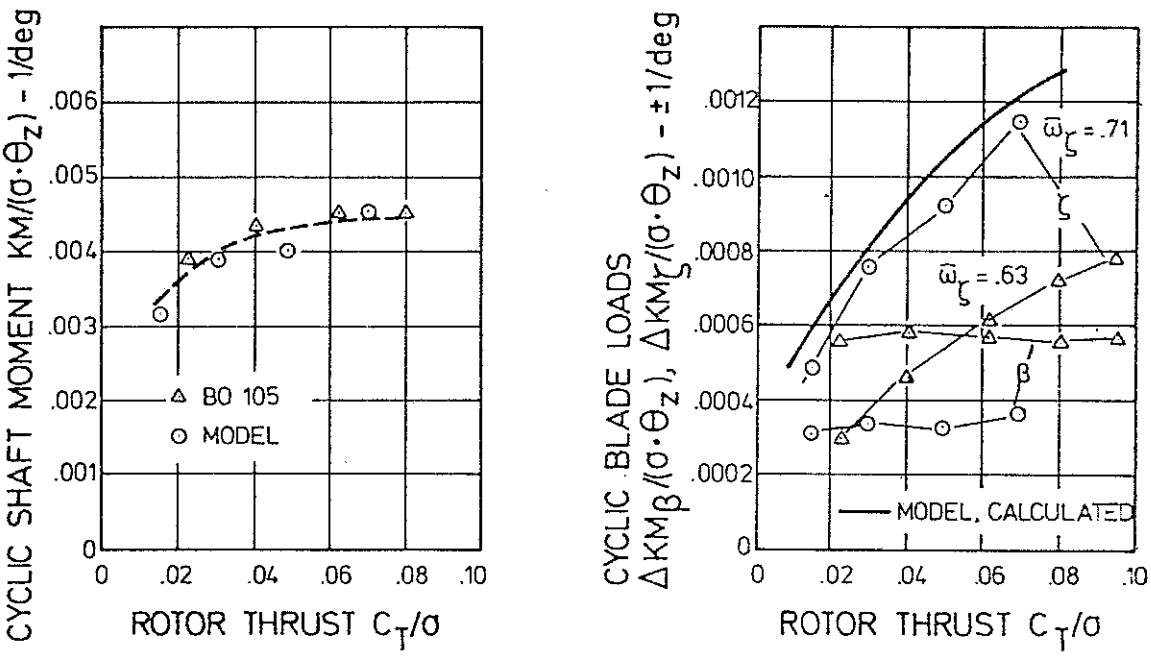

Figure 8: Cyclic shaft and cyclic 1/2-peak-to-peak flap/lag blade bending moments in hover

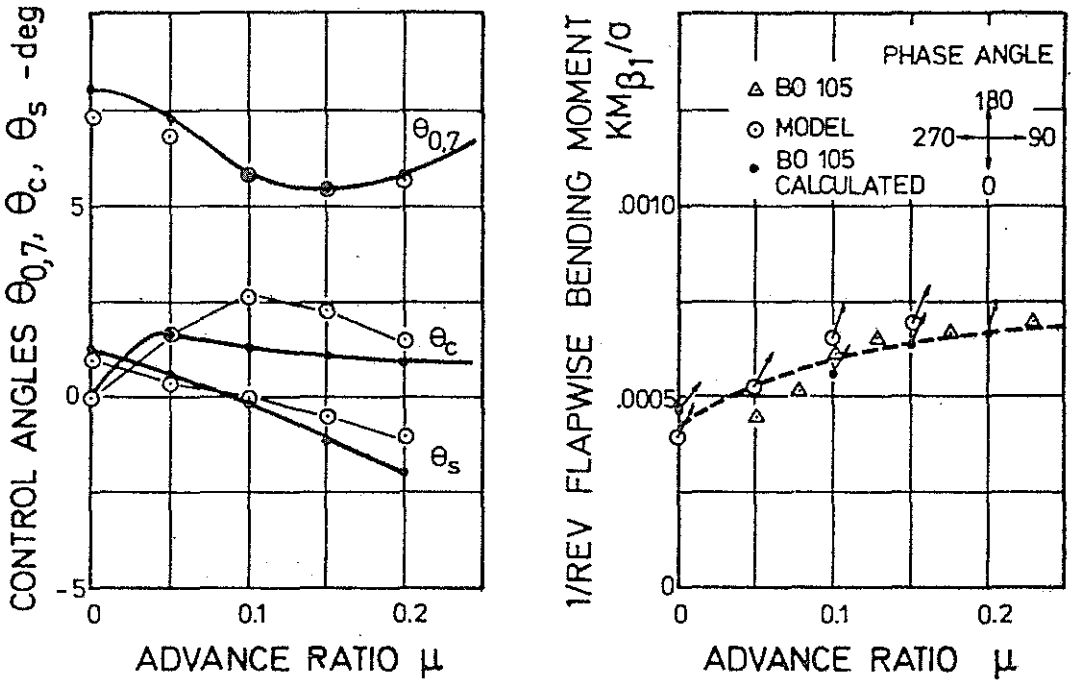

Figure 9: Control angles and 1/REV flapwise blade bending moments vs. μ in level flight

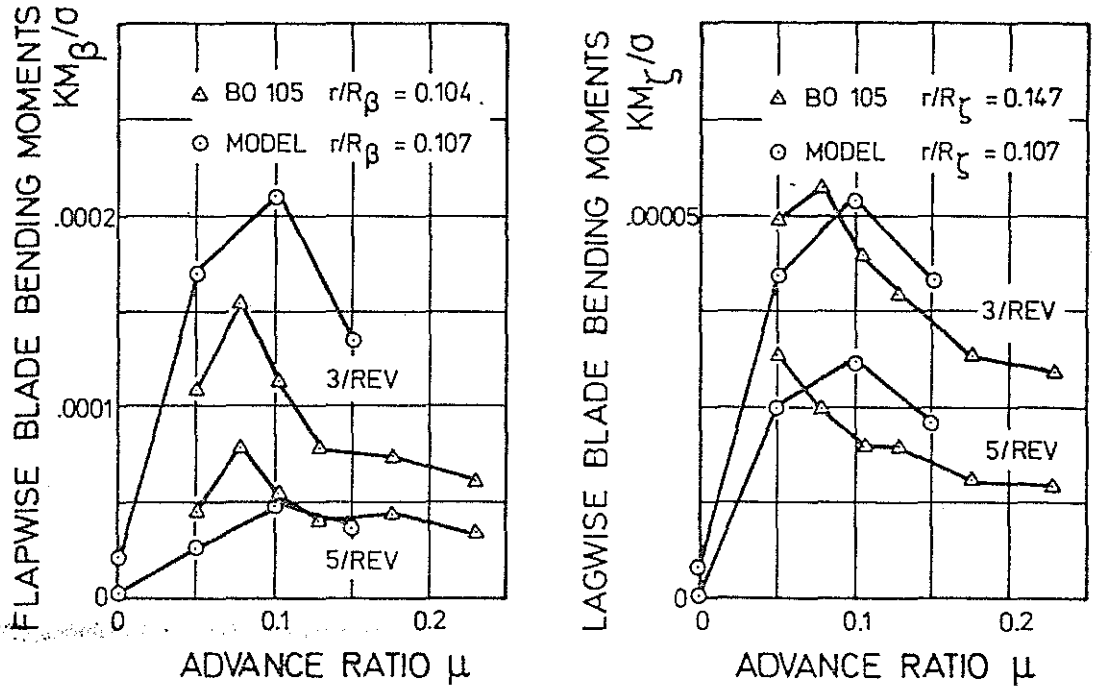

Figure 10: 3/REV and 5/REV flap/lag blade bending vs. μ in level flight

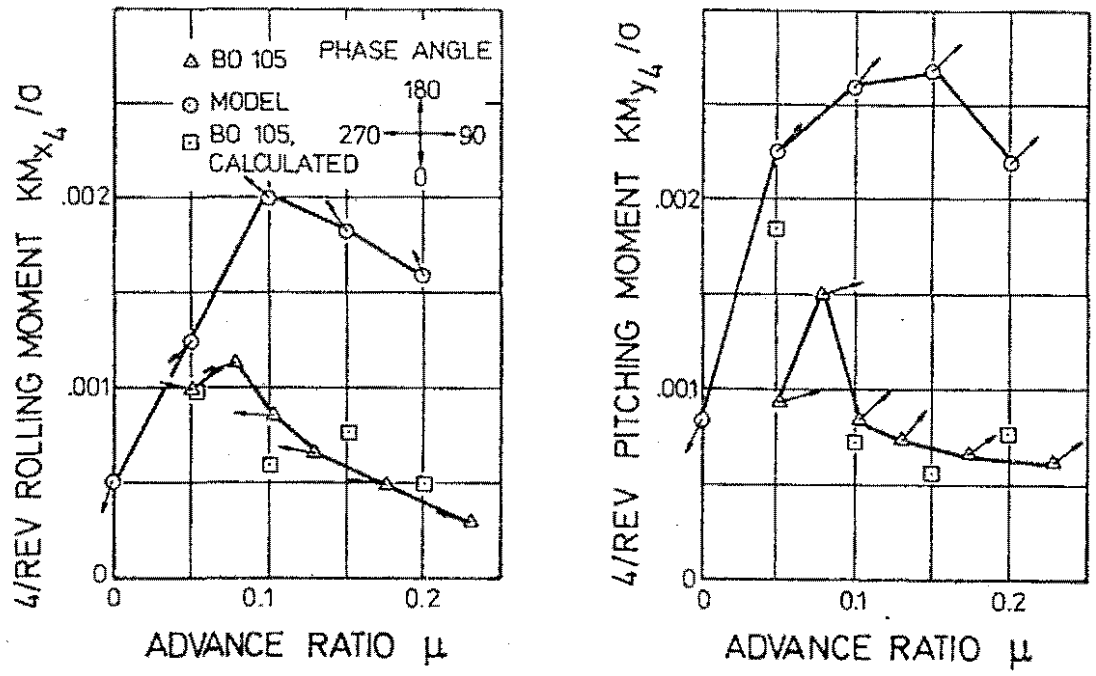

Figure 11: Rotor hub 4/REV oscillatory moments vs. μ in level flight

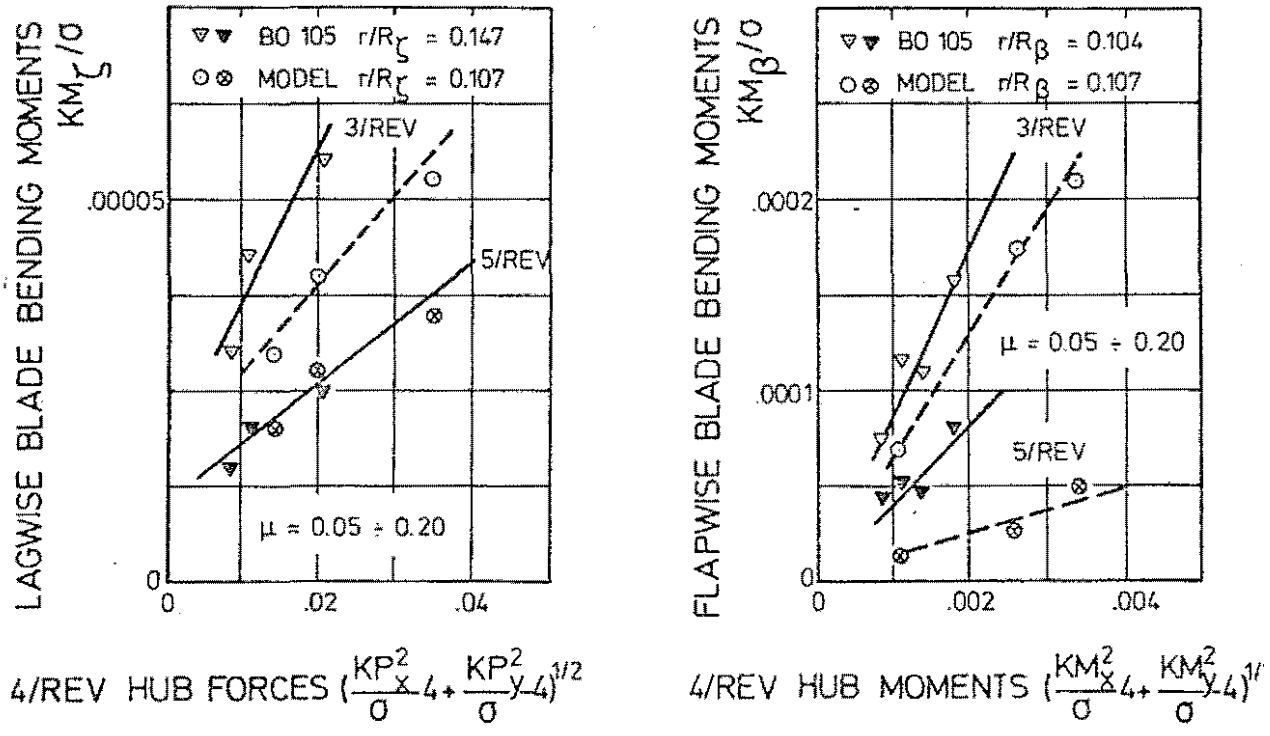

Figure 12: Crossplot of 3/REV and 5/REV lag/flap blade bending moments vs. 4/REV rotor hub forces and moments

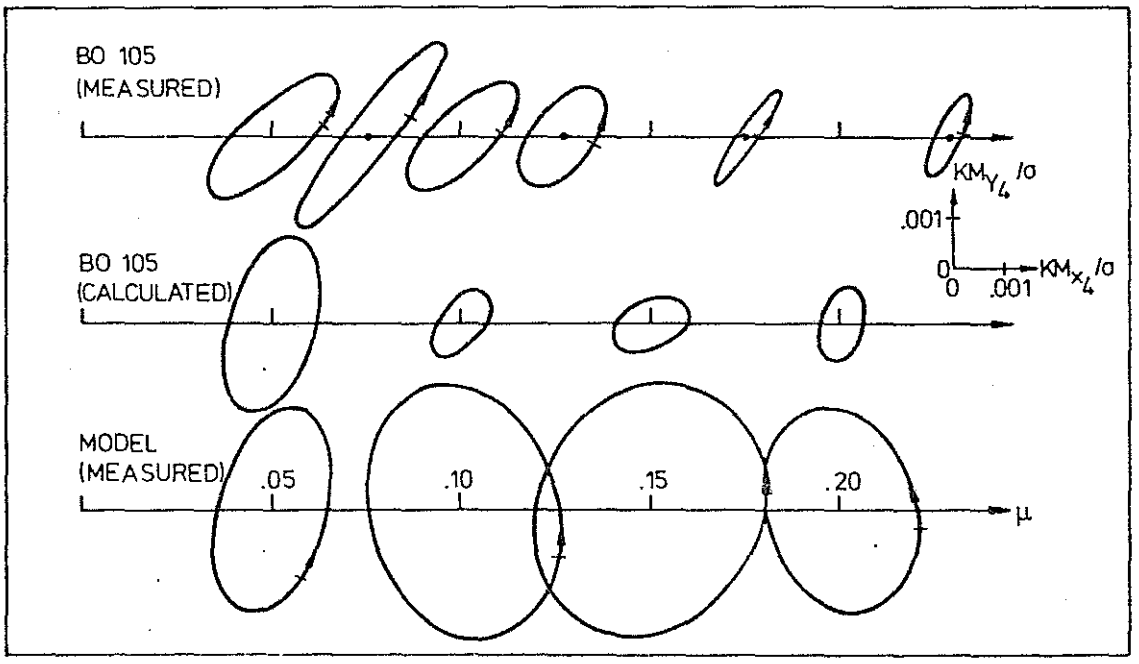

Figure 13: Rotor hub 4/REV oscillatory moments vs. μ in level flight